

## A New Insight into the Content Effect of Fluoroethylene Carbonate as a Film Forming Additive for Lithium-Ion Batteries

Xing Zhao<sup>1,2</sup>, Quan-Chao Zhuang<sup>1,\*</sup>, Shou-Dong Xu<sup>1</sup>, Ya-Xi Xu<sup>1</sup>, Yue-Li Shi<sup>1</sup>, Xin-Xi Zhang<sup>2</sup>

<sup>1</sup>Lithium-ion Batteries Laboratory, School of Materials Science and Engineering, China University of Mining and technology, Xuzhou 221116, China;

<sup>2</sup>School of Chemical Engineering and Technology, China University of Mining and technology, Xuzhou 221116, China

\*E-mail: [zhuangquanchao@126.com](mailto:zhuangquanchao@126.com)

*Received: 24 November 2014 / Accepted: 28 December 2014 / Published: 19 January 2015*

The impact of various concentrations of fluoroethylene carbonate (FEC) on the electrochemical performance of mesophase-pitch-based carbon fibers (MCF) in ethylene carbonate (EC)-based electrolyte for lithium-ion batteries is investigated using cyclic voltammetry (CV) and charge-discharge test. As expected, adding increased concentrations of FEC (up to 1 vol%) to the control electrolyte resulted in better electrolyte conductivity, cycling performance and reversible capacity. However, high concentrations of FEC lead to the deterioration of electrochemical performance. Electrochemical impedance spectroscopy (EIS) combining with Scanning electron microscopy (SEM), Fourier transform infrared (FTIR) and X-ray photoelectron spectroscopy (XPS) spectroscopy are used in order to better understand the failure mechanisms of graphite electrode in electrolytes with high concentrations of FEC. The results reveal that the deterioration of electrochemical performance is mainly due to the poor cohesion and flexibility of the solid electrolyte interphase (SEI) film formed on the graphite electrode which leads to larger charge transfer resistance as well as the SEI film resistance. Understanding how varying amounts of FEC impact cell lifetime and impedance allows for optimized electrolyte formulations to be found for different applications that may balance lifetime and power demands.

**Keywords:** Lithium-ion battery; Mesophase-pitch-based carbon fibers electrode; Solid electrolyte interphase film; Fluoroethylene carbonate; Electrochemical impedance spectroscopy

### 1. INTRODUCTION

Lithium-ion batteries have been widely used for portable electronics and more recently are finding usage in transportation applications owing to their high energy densities, long cycle life and

environmental friendliness [1-3]. At present, graphite is the most widely adopted anode material in commercial lithium-ion batteries due to its high specific capacity, low working potential close to that of lithium metal, and superior cycling behavior[4]. It is generally known that during the first intercalation of lithium into the graphite electrode, the compositions of electrolyte solution are reduced to form a surface film on graphite electrode that is commonly called the solid electrolyte interphase (SEI) [5-7]. The formation of SEI film would inevitably lead to an irreversible capacity loss during the initial charge/discharge cycle of the lithium-ion cells [8]. However, if the SEI film is steady enough, the SEI film can suppress any further electrolyte decomposition and avoids the exfoliation of the graphite structure [9]. In addition, it allows the passage of lithium ions which is the key for the achievement of a good reversibility of the battery even for prolonged cycling.

Much research has been published on the film forming additives because of the critical influences on the performance of lithium-ion batteries [5]. Up to now, many film forming additives such as vinylene carbonate (VC) [10, 11], SO<sub>2</sub> [12], Li<sub>2</sub>CO<sub>3</sub> [13-15], K<sub>2</sub>CO<sub>3</sub> [16, 17], ethylene sulfite (ES)[18], propylene sulfite (PS) [19], vinyl ethylene sulfite (VES) [20] and vinylethylene carbonate (VEC) [21-25] were successfully used in improving the electrochemical performance and modifying the surface chemistry of graphite or Si anodes for lithium-ion batteries.

As a film forming additive, the structure of fluoroethylene carbonate (FEC) is similar to ethylene carbonate (EC). A fluorine atom takes the place of a hydrogen atom which connects to the cyclic carbonate and the electronegativity of fluorine is stronger than hydrogen, which is easy to attract electrons, so the reductive decomposition of FEC to form SEI film can occur at higher potential than that of EC.

In the past few years, FEC was reported a lot as electrolyte additive, mainly for cathode materials such as LiMn<sub>2</sub>O<sub>4</sub> [26] and Li<sub>2</sub>CoO<sub>2</sub> [27] to high/low temperature performances modified, for anode material Si [28, 29], graphite [30, 31] and Li-S cells [32] to improve the properties of SEI film, for a graphite anode to demonstrate the effect of FEC on the cycling performance of a lithium-ion battery[33], for graphite anodes at elevated temperatures to describe the role of FEC on the thermal behaviors [34], or for Na-ion batteries[35]. Now, FEC has been widely used as a film formation additive in commercial electrolyte, however, the content of FEC adding in EC-based electrolyte is commonly operating by experience, the effect of the content of FEC on the electrochemical properties of graphite anode as well as the surface film formation is still not clear, and even the effect of the content of FEC on the conductivity of the electrolytes are rarely reported. Thus, whether is there an optimal concentration? And if there is an optimal concentration, what is the failure mechanism of graphite electrode in the case of excessive addition of FEC? As for our knowledge, the above questions have not been known until now. The optimal concentration of FEC is highly application dependent, but understanding the impact of adding FEC at various percentages will lead to the ability to better optimize electrolyte formulations for the demands of different applications.

Herein, the electrochemical behaviors of MCF electrode in 1M LiPF<sub>6</sub> dissolved in EC/diethyl carbonate (DEC)/dimethyl carbonate (DMC) (1:1:1, v/v/v) electrolyte with and without FEC were investigated using charge/discharge tests and cyclic voltammograms(CV). Scanning electron microscopy (SEM) combining with XPS techniques were used to investigate the effect of FEC on the morphology and surface chemistry of the SEI film. To elaborate the film-forming properties and

failure mechanism of MCF electrode in the FEC-containing electrolyte, electrochemical impedance spectroscopic (EIS) measurement, which is one of the most powerful tools to analyze electrochemical processes occurring at electrode/electrolyte interfaces and has been widely applied to the analysis of electrochemical lithium intercalation into carbonaceous materials including graphite [36-43], was applied.

## 2. EXPERIMENTAL

### 2.1 Preparation of the graphite electrode

The graphite electrode used in this study was prepared by spreading a mixture comprising, by weight, 90 % MCF (Petoca, Japan) and 10 % PVdF (HSV910, USA) binder dissolved in N-methyl-2-pyrrolidone (NMP, Alfa Aesar, A. Johnson Matthey Company, China) onto a copper foil current collector.

### 2.2 Electrochemical measurement

CV and EIS were carried out by a three-electrode glass cell with Li foils as the counter and reference electrode using an electrochemical workstation (CHI660D, Chenhua Co., Shanghai, China) at room temperature, and the area of the work electrode is  $1.5 \times 1.5 \text{ cm}^2$ . Charge-discharge test was evaluated using CR2025-type coin cell. Coin cell was assembled with a graphite working electrode and a Li foil counter electrode, separated by a polypropylene microporous separator (Celgard 2400) soaked in electrolyte. The electrolyte was 1M LiPF<sub>6</sub> dissolved in EC/ DEC/ DMC (1:1:1, v/v/v, Shanshan Inc., China). FEC (Provided by Shanshan Inc., China) as an electrolyte additive was added at different volume ratio (0.5, 1.0, 3.0, 5.0 and 10.0 %) with the above electrolyte. CV was measured at a scan rate of  $0.5 \text{ mV} \cdot \text{s}^{-1}$  in the potential range of 3.0-0.0 V (vs. Li/Li<sup>+</sup>). EIS was measured over the frequency range from  $10^5$  to  $10^{-2}$  Hz with a potentiostatic signal amplitude of 5 mV. The electrode was equilibrated for 1 h before the EIS measurements, in order to attain steady-state conditions. And the obtained impedance results were fitted using Zview software. The coin cells were galvanostatically charged and discharged in a battery analyzers (Neware, Shenzhen, China) over a range of 1.5-0.001 V vs. Li/Li<sup>+</sup> at a constant current density of 0.1 C (1C=372 mA g<sup>-1</sup>).

### 2.3 SEM, XPS and FTIR measurements

The specimen after CV test was transferred into the glove box and scraped from the copper foil current collector, washed in DMC and dried under vacuum to remove the residual electrolyte. The change in morphology of the graphite electrode before and after electrochemical tests in different electrolyte compositions was investigated by a LEO 1530 Field Emission Scanning Electron Microscopy (FE-SEM, Oxford Instrument). The components of the surface film formed on cycled

electrodes were characterized by XPS (ESCALAB 250XI, Thermo Scientific, USA) and FTIR (Tensor-27, BRUKER) using a pellet containing a mixture of KBr in the range of 4000~650 cm<sup>-1</sup>.

### 3. RESULTS

#### 3.1 The conductivity of the electrolytes

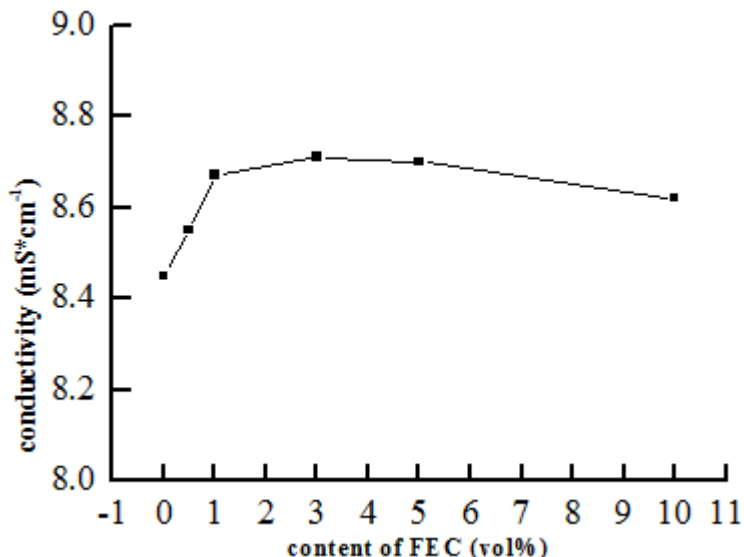


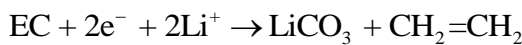
**Figure 1.** Variation of the conductivity of the electrolytes ( $1 \text{ mol}\cdot\text{L}^{-1}$  LiPF<sub>6</sub> in EC: DEC: DMC (1:1:1, v/v/v)) with the content of FEC

The conductivity of the electrolytes varying with the content of FEC is investigated and the results are shown in Fig. 1. It can be seen that with the increase of the content of FEC, the conductivity of the electrolytes first increase rapidly from 0 % to 1 % and then decrease slowly from 3 % to 10 %, but the conductivity of the electrolytes still larger than that of the electrolyte without FEC even when the content of FEC reach to 10 %.

#### 3.2 CV Results

Cyclic voltammograms of graphite electrodes in the electrolytes of  $1 \text{ mol}\cdot\text{L}^{-1}$  LiPF<sub>6</sub> in EC: DEC: DMC (1:1:1, v/v/v) and with different volume ratio (0.5, 1.0, 3.0, 5.0 and 10.0 vol%) of FEC additive are presented in Fig. 2. For the electrode cycled in FEC-free electrolyte, as can be seen in Fig. 2(a), there are two reductive current peaks (peak  $\alpha$  at the voltage around 0.8 V and  $\beta$  around 0.5 V) can be observed in the first lithium ion insertion process. After the first cycle, peaks  $\alpha$  and  $\beta$  disappear, implying that peaks  $\alpha$  and  $\beta$  are attributed to the formation of the SEI film on the surface of the graphite. According to Naji et al. [44, 45], the reduction process of EC mainly includes two steps.

The first step (single electron reduction process):



The second step (double electrons reduction process):

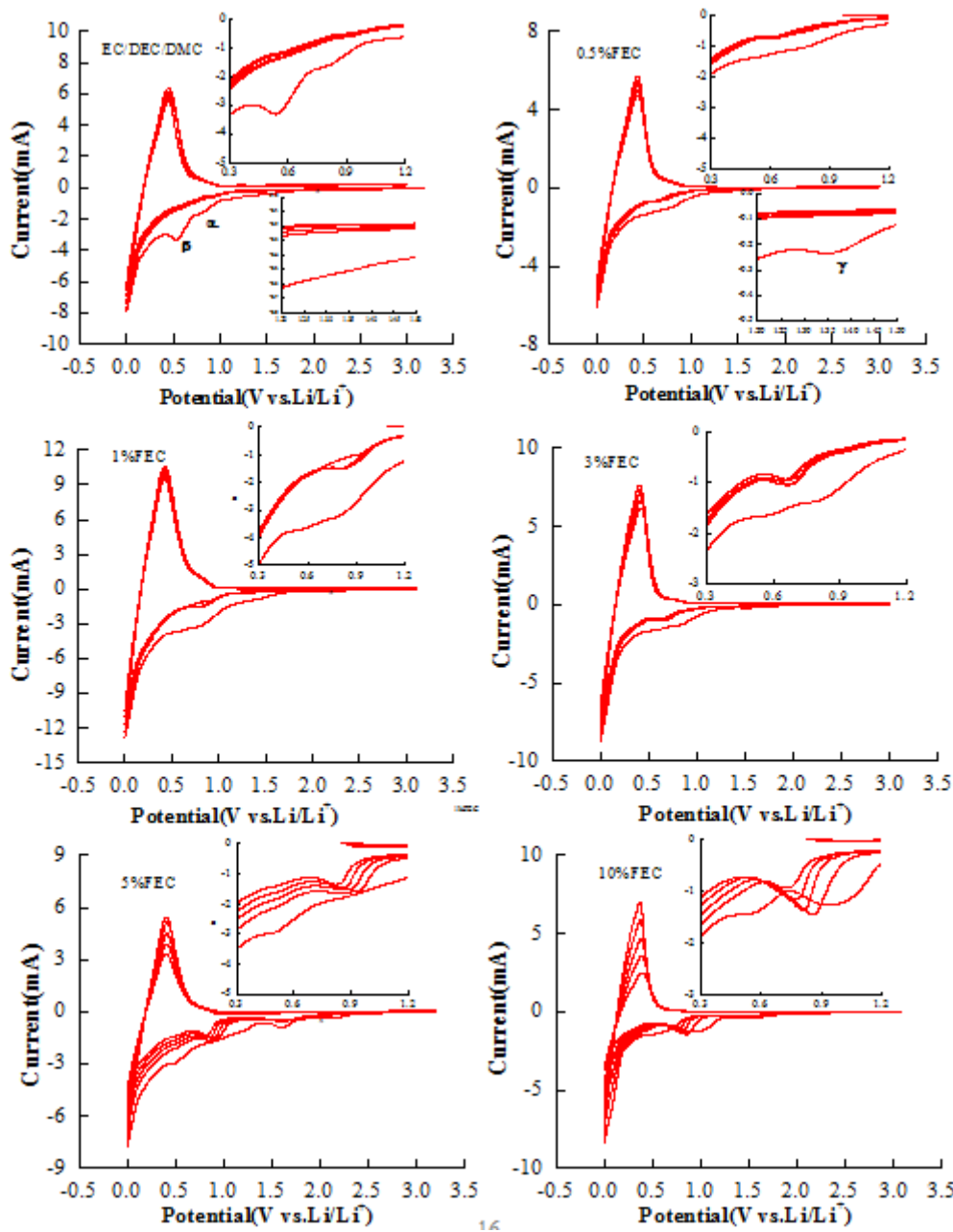
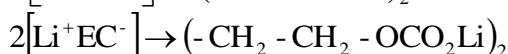
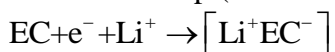


**Figure 2.** Cyclic voltammetry recorded on graphite electrode in a three-electrode glass cell using the electrolyte with different contents of FEC

Thus, it can be proposed that peak  $\alpha$  is attributed to the reduction of EC into  $\text{Li}_2\text{CO}_3$  and peak  $\beta$  is associated with EC reduced into alkyl lithium carbonate ( $\text{ROCO}_2\text{Li}$ ). A pair of reduction and

oxidation peaks are found around 0.0 and 0.3 V, respectively, indicating that the processes of lithium-ion insertion and extraction.

As shown in Fig 2(b), after 0.5 vol% FEC was added into the electrolyte, the peak  $\beta$  is greatly weakened and a new reduction peak,  $\gamma$ , which could be assigned to the formation of SEI film due to the reductive decomposition of FEC, is observed in the potential region from 1.4 to 1.3 V, which indicate that the formation of lithium alkyl carbonate due to the double electrons reduction process of EC is strongly suppressed. Moreover, the CV curves of graphite electrode in the 0.5 % FEC-containing electrolyte show good coincidence. But when the content of FEC reaches to 3.0 %, the coincidence of the CV curves deteriorate, and even worse as the content of FEC continue increasing. An abnormal phenomenon can be found that peak  $\alpha$  still exists and become more apparent as the increase of the content of FEC after the first cycle, which indicate the unstable performance of SEI film. This phenomenon may be due to that the SEI film breakdown during the processes of lithium-ion insertion and extraction, then the new SEI film form on the fresh surface of graphite which will inevitably lead to more and more irreversible loss of capacity of the lithium-ion batteries during charge-discharge cycles.

### 3.3 Charge-discharge test

The charge/discharge curves and cyclic performance of the graphite electrode in electrolytes without and with different volume ratio (0, 0.5, 1.0, 3.0 and 5.0 vol%) of FEC additive are displayed in Fig. 3 and Fig. 4. For the result in the electrolyte without FEC, it can be seen from Fig. 3 (a), the slowly decreasing potential starts from about 1.0 V, and forms a potential plateau in the potential range of 1.0-0.5 V in the first lithium-ion insertion process, which is obviously attributed to the reduction of EC to form SEI film with a discharge capacity of about  $30 \text{ mAhg}^{-1}$ , corresponding to the CV results. But in the electrolyte with FEC, the slope  $\varepsilon$ , which appears in the potential range of 0.8-0.5 V in the FEC free electrolytes, disappears. Thus, the slope  $\varepsilon$  can be attributed to the reduction of EC into  $\text{ROCO}_2\text{Li}$  with a discharge capacity of about  $15 \text{ mAhg}^{-1}$ , and its disappearing displays the strong inhibition of this process. With the increase of FEC, the start potential of the plateau increases to 1.5 V, which can be ascribed to the reduction of FEC to form SEI film.

Fig. 4 shows the cyclic performance of the graphite electrode in electrolytes without and with different volume ratio (0, 0.5, 1.0, 3.0 and 5.0 vol%) of FEC. When the FEC content is 0.5% and 1.0 vol%, although the initial charging capacity of the battery is similar to that in the electrolyte without FEC, the cyclic performance and reversible capacity are both improved, especially for 1.0 vol% FEC. After 30 cycles, the reversible capacity of the battery in the electrolyte with 1.0 vol% FEC is  $304 \text{ mAh} \cdot \text{g}^{-1}$ , while the battery in the electrolyte without FEC is only  $293.9 \text{ mAh} \cdot \text{g}^{-1}$ . However, the reversible capacity and cyclic performance in the electrolytes with 3.0 vol % and 5.0 vol% FEC are lower than that in the electrolyte without FEC with the reversible capacity of  $260.8 \text{ mAh} \cdot \text{g}^{-1}$  and  $269.2 \text{ mAh} \cdot \text{g}^{-1}$  after 30 weeks cycle, displaying that when choosing FEC as a film-forming additives, we must control the amount of FEC in the electrolyte to achieve the best effect of improvement, and 1.0 vol % FEC may be the appropriate content.

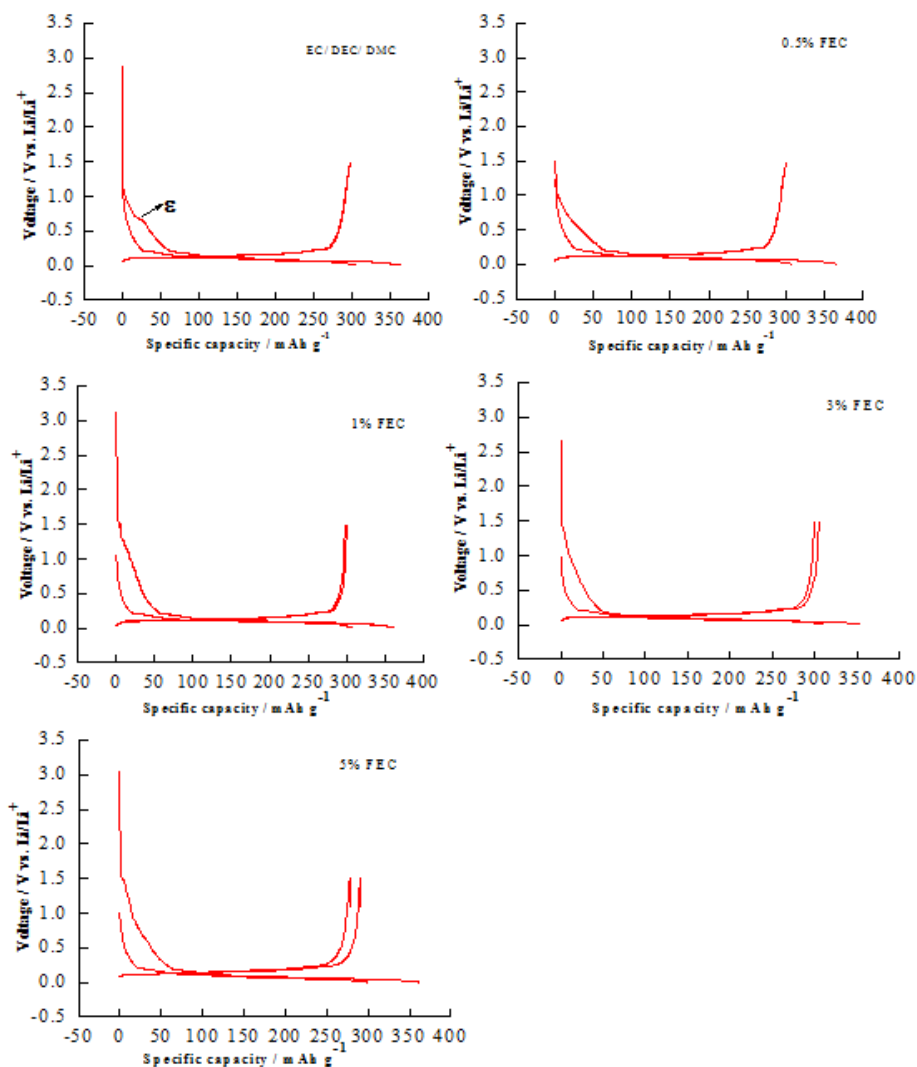


**Figure 3.** Charge-discharge characteristics of graphite electrode in the electrolytes with different contents of FEC

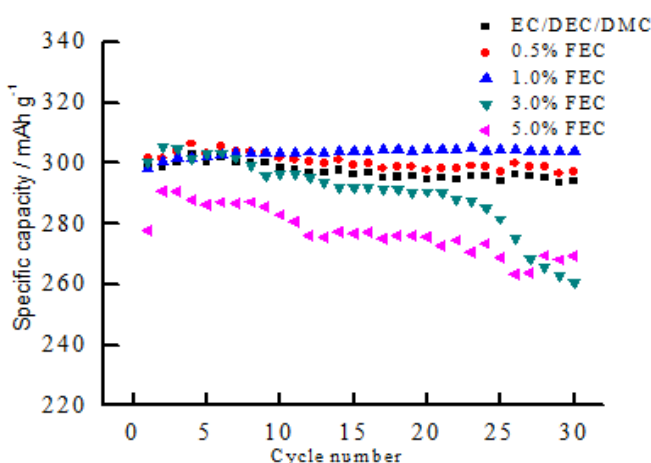
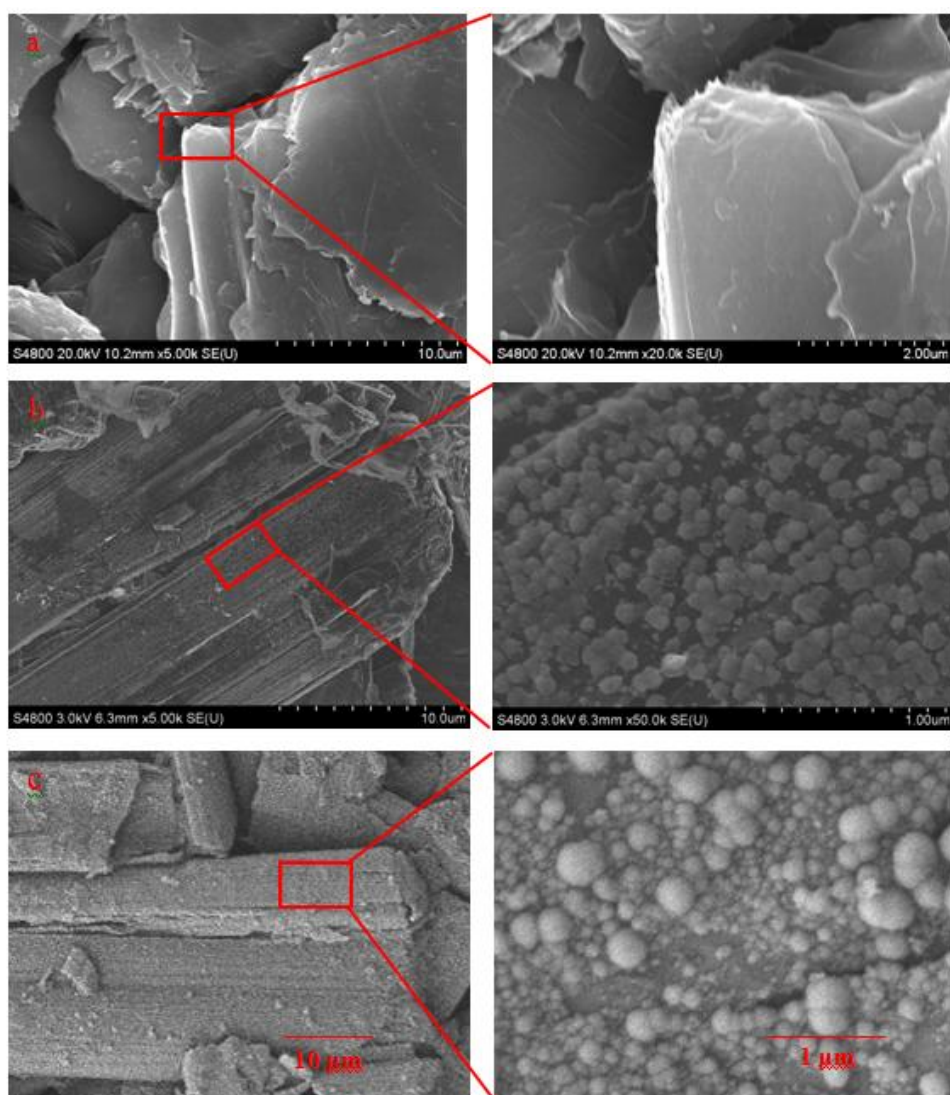


**Figure 4.** Cycle performance of graphite electrode using  $1 \text{ mol} \cdot \text{L}^{-1}$   $\text{LiPF}_6$  in EC: DEC: DMC with or without FEC

### 3.4 Surface morphology and chemical composition

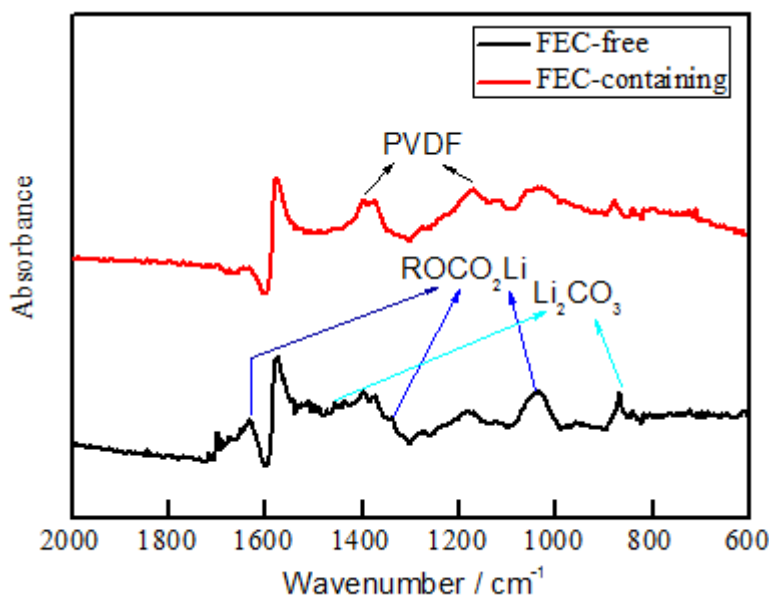
To further study of the effects of FEC on the surface chemistry and morphology of graphite electrodes, SEM, FTIR and XPS were introduced.

Fig. 5 shows the SEM images of the surface of the graphite electrode after CV test in electrolytes without, with 1.0 vol% and 10 vol% FEC. From the SEM images of the graphite electrode after CV test in FEC free electrolytes in Fig. 5 (a), it can seen that the surface of the SEI film looks relatively smooth, showing a state of an amorphous polymer. Compared with that in FEC free electrolytes, great changes take place in the SEM images of the graphite electrode after CV test in the electrolyte with 1.0 vol% FEC. The surface of the graphite particle is covered by uniform and small particles with the diameter of about 100 nm, and these small particles are evenly distributed over the surface of the electrode. But as the content of FEC in the electrolyte reaches to 10 vol%, some of the particles on the surface of graphite grows to about 300 nm and unevenly distributed.



**Figure 5.** SEM images of graphite electrode after CV cycles in (a) FEC-free (b) 1% FEC and (c) 10% FEC electrolytes

Fig. 6 shows FTIR spectra of the electrode obtained after electrochemical cycles in FEC-free and FEC-containing electrolytes. For FTIR spectrum of the electrode cycled in FEC-free electrolyte, the pronounced peaks at  $1695.6\text{ cm}^{-1}$  (vas C-H),  $1397.4\text{ cm}^{-1}$  (vs C-H) and  $1070.2\text{ cm}^{-1}$  (v C-O) are assigned to lithium alkylcarbonates ( $\text{ROCO}_2\text{Li}$ ) [21, 42], which are the major reduction products of EC solvent via the double electrons reduction process. The pronounced peaks at around  $1457.6$  and  $878.36\text{ cm}^{-1}$  (v C-O) belong to the inorganic carbonate,  $\text{Li}_2\text{CO}_3$ , which is mainly formed due to the single electron reduction process of EC.



**Figure 6.** FTIR spectra of the electrode obtained after electrochemical cycles in FEC-free and FEC-containing electrolytes

For the spectrum related to the electrode cycled in the FEC-containing electrolyte, peaks assigned to  $\text{ROCO}_2\text{Li}$  are much smaller than that of FEC-free electrolyte, indicating that the formation of  $\text{ROCO}_2\text{Li}$  due to the double electrons reduction process of EC is suppressed, in accordance with CV result.

Fig. 7 shows the XPS spectra for the surface layer formed on the graphite electrode after CV test in electrolyte without and with 1.0 vol% FEC. The strongest peak in C1s XPS spectra centered at 284.8 eV can be assigned to C-C bond in the SEI film [28], the peak centered at 290 eV is assigned to the C-O and  $\text{CO}_3^{2+}$  in the SEI film [28], and the peak centered at 286 eV is assigned to alkoxy and alkyl in the SEI film<sup>[28]</sup>. Compared to XPS spectra in FEC free electrolyte, there is a new peak at 287 eV in the electrolyte with 1.0 vol% FEC which can be assigned to the polycarbonate compounds due to the reduction of FEC.

In F1s XPS spectra, the strongest peak centered at 687.5 eV in the FEC free electrolyte can be assigned to PVDF binder [46], and a shoulder at 685 eV is assigned to LiF. However, the strongest

peak in the electrolyte with 1.0 vol% FEC appears at 685 eV, indicating that LiF is an important product for the formation of the SEI film in the FEC-containing electrolyte.

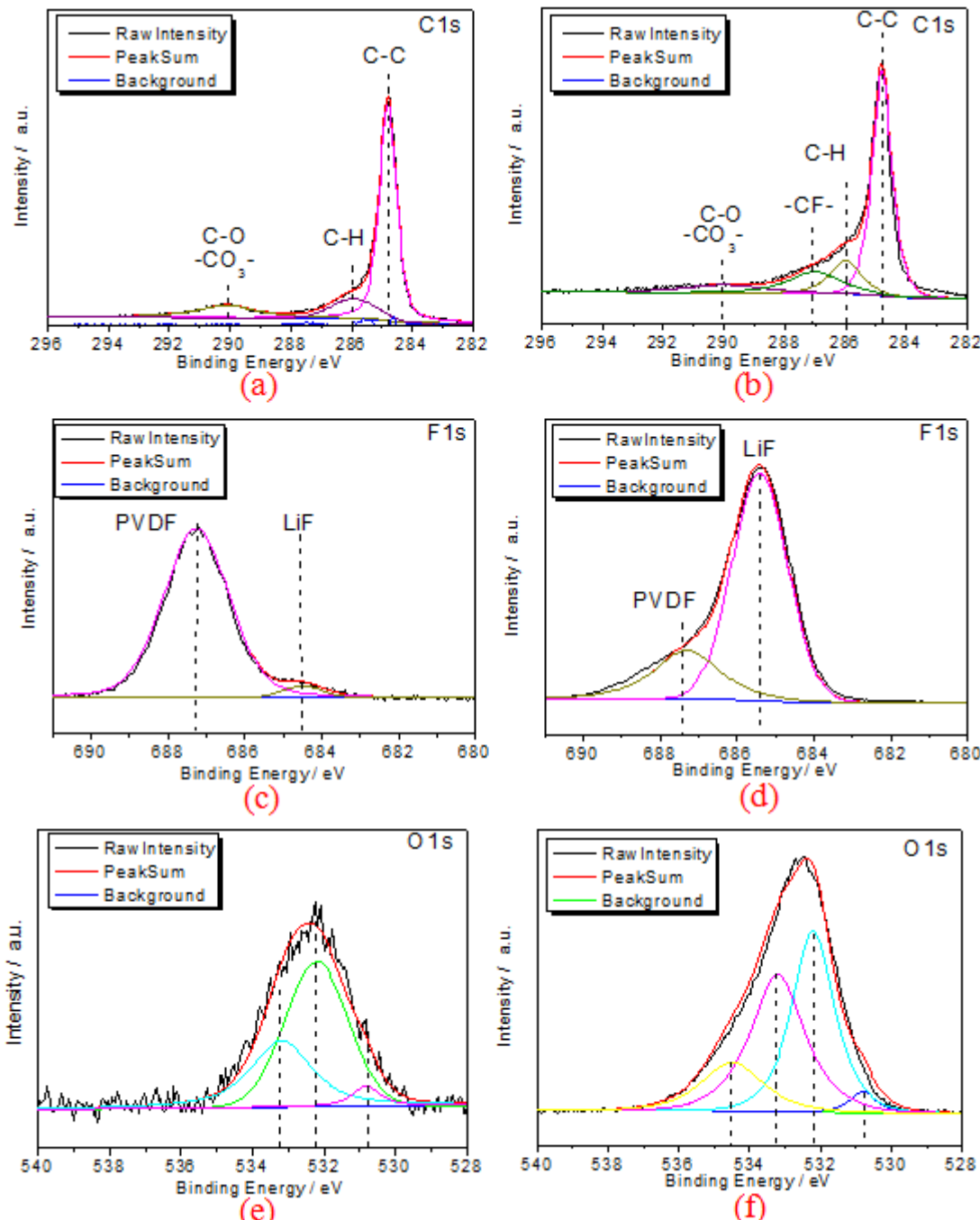


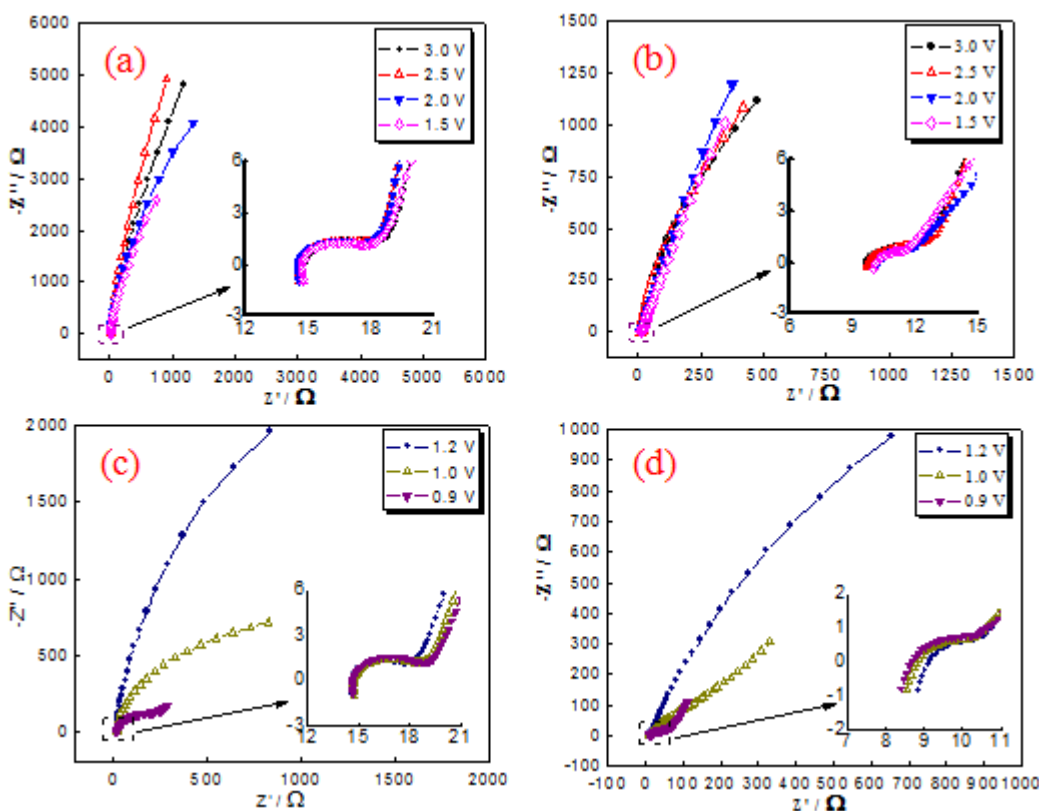
**Figure 7.** C 1s, F 1s and O 1s XPS spectra of graphite electrodes after electrochemical cycles in FEC-free electrolyte ((a), (c), (e)) and FEC-containing electrolyte ((b), (d), (f))

There are three peaks centered at 530.8, 532.2, 533.2 respectively in O1s XPS spectra assigned to Li<sub>2</sub>CO<sub>3</sub> and alkyl lithium carbonate due to the reduction of EC [28]. Compared to XPS spectra in FEC free electrolyte, the new peak centered at 534.5 eV in the electrolyte with 1.0 vol%

FEC can be assigned to polycarbonate compounds due to the reduction of FEC [47], in accordance with C1s XPS results.

### 3.5 EIS characterizations

EIS is one of the most powerful tools to analyze electrochemical processes occurring at electrode/electrolyte interfaces, and has been widely applied to the analysis of electrochemical lithium intercalation into carbonaceous materials including graphite [48, 49], so EIS measurements were performed on the graphite electrode during the process of the first lithium ion insertion. Fig. 8 and 9 depict the Nyquist plots of the graphite electrodes at various potentials from 3.0 to 0.1 V during the first lithium-ion insertion process in the electrolytes without FEC, with 1% FEC and 10% FEC. At open-circuit voltage (OCV) 3.0 V, as can be seen in Fig. 8 (a)-(b) and Fig. 9 (a), the impedance spectroscopy of the graphite electrodes are similar, all of them show a small semicircle in high-frequency region and a sloping line in low-frequency region. Because there is no SEI film formed at 3.0 V, the high frequency semicircle should be assigned to the contact problems that may relate to the contact between the electrolyte and graphite, or graphite and graphite in the electrode bulk, as suggested by Holzapfel et al. [50]. The sloping line represents the retardance characteristic of graphite electrode [51]. with the electrode polarization potential changing from OCV to 2.0 V, the Nyquist plots does not change much in the electrolytes without FEC, with 1% and 10% FEC, and no important modification of the impedance spectroscopy can be observed.



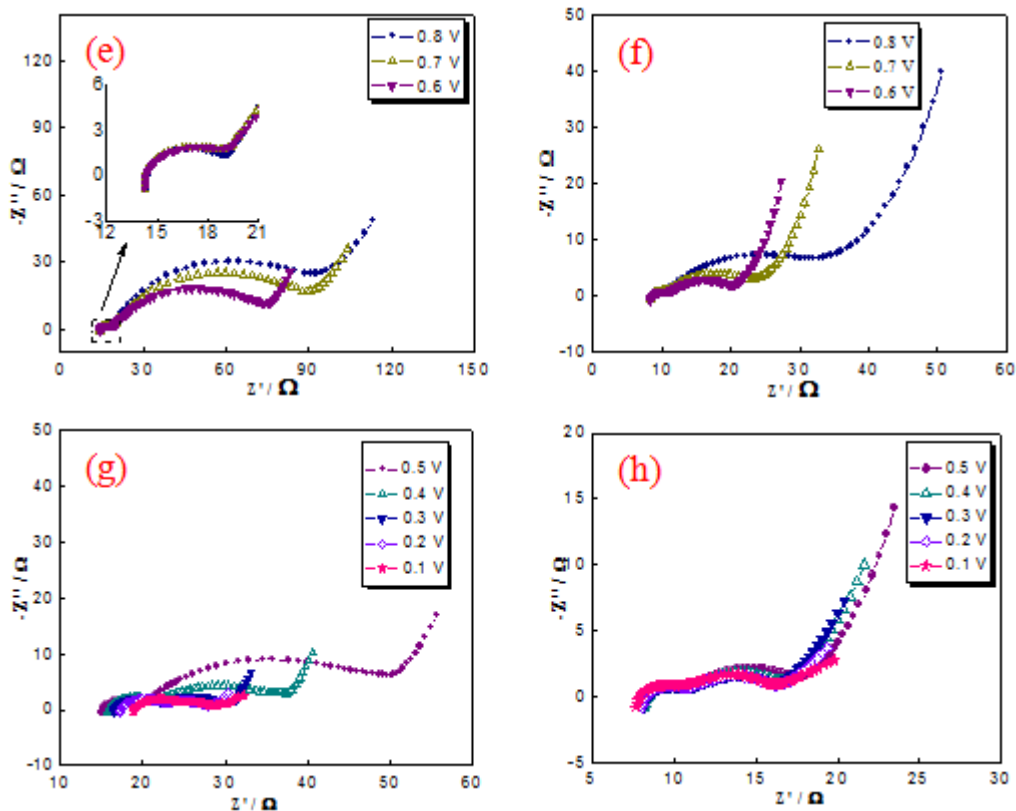


**Figure 8.** Nyquist plots of the graphite electrode at various potentials from 3.0 to 0.1 V during the first lithium ion insertion process in (a), (c), (e) and (g) FEC-free electrolyte, (b), (d), (f) and (h) 1% FEC electrolyte

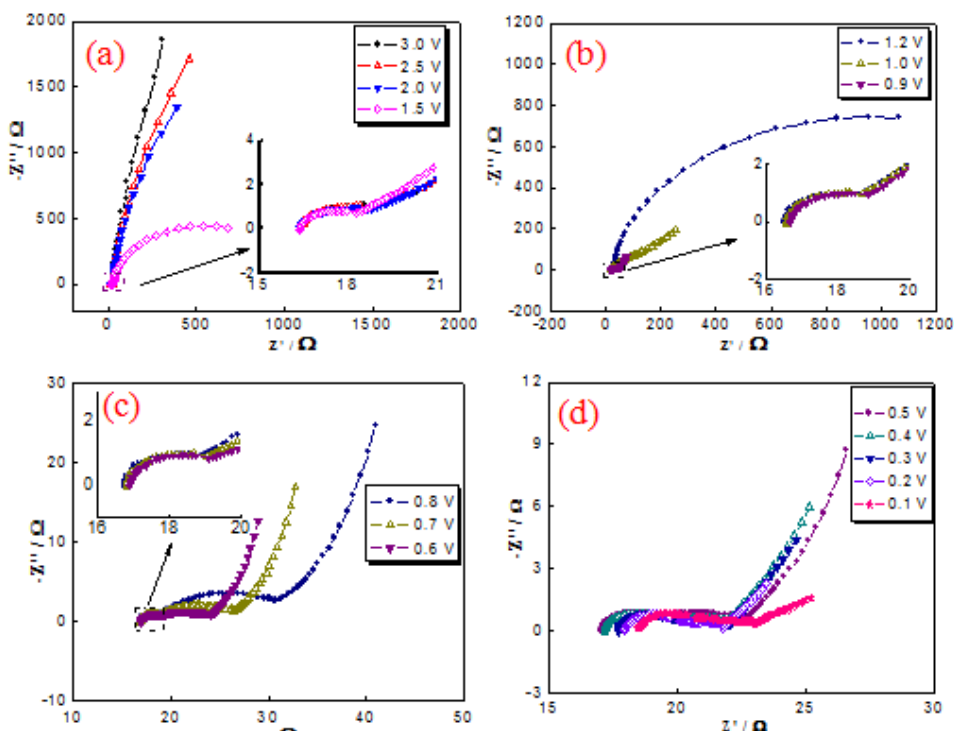


**Figure 9.** Nyquist plots of the graphite electrode at various potentials from 3.0 to 0.1 V during the first lithium ion insertion process in 10% FEC electrolyte

Along with the further decrease of the electrode potential, the sloping line which is strongly potential-dependent bends toward the real axis and forms a semicircle at 1.0 V, then turns into a semicircle in the middle-frequency and an inclined line in the low frequency at 0.9 V in the FEC free electrolytes. Nevertheless, the sloping line forms a semicircle at 1.5 V in the electrolytes FEC with 10% FEC, and evolves into a semicircle in the middle-frequency and an inclined line in the low frequency at 1.0 V in the electrolytes with 1% and 10% FEC which is higher than that in the FEC free electrolytes, implying that the reductive decomposition of FEC to form SEI film can occur at higher potential than that of EC. When the potential drops to 0.8 V, the Nyquist plots for all electrodes are consisted of three parts, essentially two semicircles and one line. According to Aurbach et al. [52-54], the semicircle in the high-frequency region (high-frequency semicircle, abbreviated as HFS) is usually attributed to the SEI film covering on the graphite electrode, the semicircle in the middle-frequency region (middle-frequency semicircle, abbreviated as MFS) is ascribed to charge transfer process at the electrolyte/electrode interface, and the inclined line in the low-frequency region is attributed to solid-state diffusion of the lithium-ion in the graphite matrix. Considering the truth that there has been an initial semicircle in the high-frequency region when the potential is above 1.0 V, here HFS should be related to not only the contact problems but also the migration of lithium-ion through SEI film.

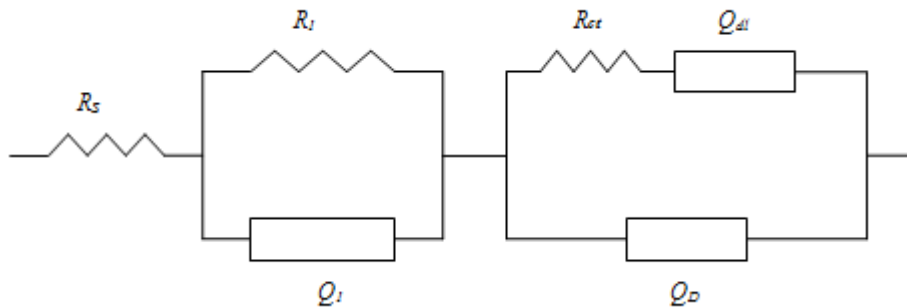


**Figure 10.** Equivalent circuit proposed for fitting impedance spectra of graphite electrode during the first lithium-ion insertion process

According to the experimental results obtained in this work and our previous study on graphite electrode [17, 55-56], an equivalent circuit, as shown in Fig. 10, is proposed to fit the impedance spectra of the graphite electrode in FEC-containing and FEC-free electrolytes in the first lithium-ion insertion process. The resistance-capacitance (RC) circuit signifies the semicircle in the Nyquist plots of the EIS. CPE is a constant phase element, and CPE is used instead of capacitance in this study.  $R_s$  is the Ohmic resistance;  $R_I$  is the uncompensated resistance, including the resistance of SEI and contact problems.  $R_{ct}$  and  $Q_{dl}$  represent the charge-transfer resistance and the double-layer capacitance in the middle-frequency region. The low-frequency region, however, cannot be modeled properly by a finite Warburg element. We have chosen, therefore, to replace the finite diffusion by a CPE, that is,  $Q_D$ . This approach has been used to characterize the graphite electrode [41] and has allowed us to obtain a good superposition with the experimental data.

### 3.6 Variations of $R_1$ with the electrode potential in the high-frequency region

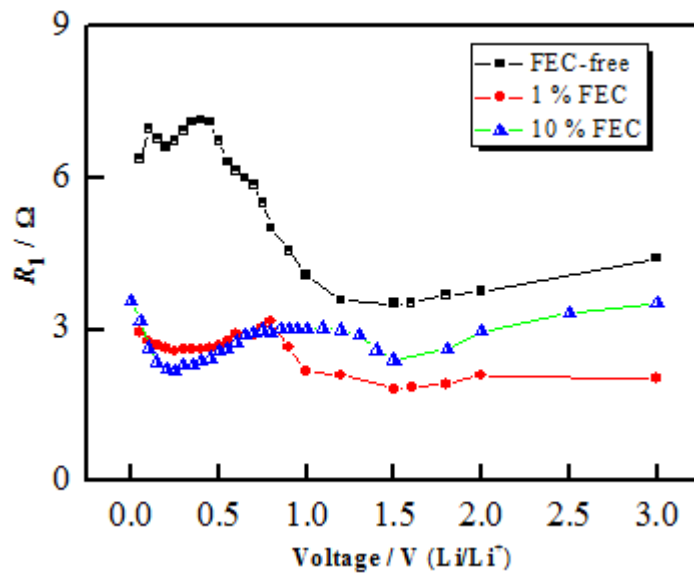


**Figure 11.** Variation of  $R_1$  with the electrode potential in FEC-free, 1% FEC and 10% FEC electrolytes

Variations of  $R_1$  with electrode potential obtained from fitting the experimental impedance spectra of the graphite electrode in the first lithium insertion process in FEC-free, 1 % FEC and 10 % FEC electrolytes are displayed in Fig. 11. In FEC-free electrolyte,  $R_1$  remains almost invariant with electrode polarization potential decreasing from 3.0 to 1.1 V. Here,  $R_1$  could only be attributed to the contact resistance, as discussed above. On charging from 1.1 to 0.5 V,  $R_1$  increases rapidly, indicating the SEI film begin to form and signifying the increase of the thickness of the SEI film. When the electrode potential is changed from 0.5 to 0.2 V,  $R_1$  decreases rapidly, which may be ascribed to that the reduction products of EC, such as alkyl lithium carbonate, react with the trace amount of water to form a composition with better lithium ion conducting property [17], resulting in the SEI film containing more inorganic salts. With the potential changing from 0.2 to 0.05 V,  $R_1$  increases again, this may be attributed to the processes of the cracking and repairing of the SEI film [17], which will be discussed below.

In 1% FEC electrolyte, on charging from 3.0 to 1.5 V,  $R_1$  has a similar trend with that in FEC-free electrolyte. With the electrode polarization potential changing from 1.5 to 1.0 V,  $R_1$  increases gradually, reflecting the SEI film due to the reduction and polymerization of FEC begin to form. On further charging from 1.0 to 0.8 V,  $R_1$  increases rapidly, implying the increase of the thickness of the SEI film due to the single electron reduction process of EC to form  $\text{Li}_2\text{CO}_3$  [45]. On further charging to 0.5 V,  $R_1$  decreases slowly, which is different from that in FEC-free electrolyte, implying that the reduction and polymerization of EC via double electrons reduction process has been inhibited, corresponding to the CV and charge-discharge results. On further charging from 0.5 to 0.05 V,  $R_1$  behaves like in the FEC-free electrolyte. In addition,  $R_1$  in 1% FEC electrolyte are smaller than that in

FEC-free electrolyte in the whole lithium insertion process, designating that the SEI film formed in 1% FEC electrolyte is thinner and better conductivity than that in FEC-free electrolyte.

When the content of FEC reaches to 10 %, with the electrode polarization potential changing from 1.5 to 1.2 V,  $R_I$  increases, reflecting that the SEI film forms on the graphite electrode due to the reduction decomposition of FEC. On charging from 1.2 to 0.7 V,  $R_I$  keeps almost invariable, which is different from that in FEC-free and 1% FEC electrolyte, indicating that the reduction decomposition of EC via single and double electrons reduction processes both have been inhibited. On further charging to 0.05 V,  $R_I$  behaves like in the FEC-free and 1% FEC electrolyte.

### 3.7 Variation of $R_{ct}$ with electrode potential in the middle-frequency region

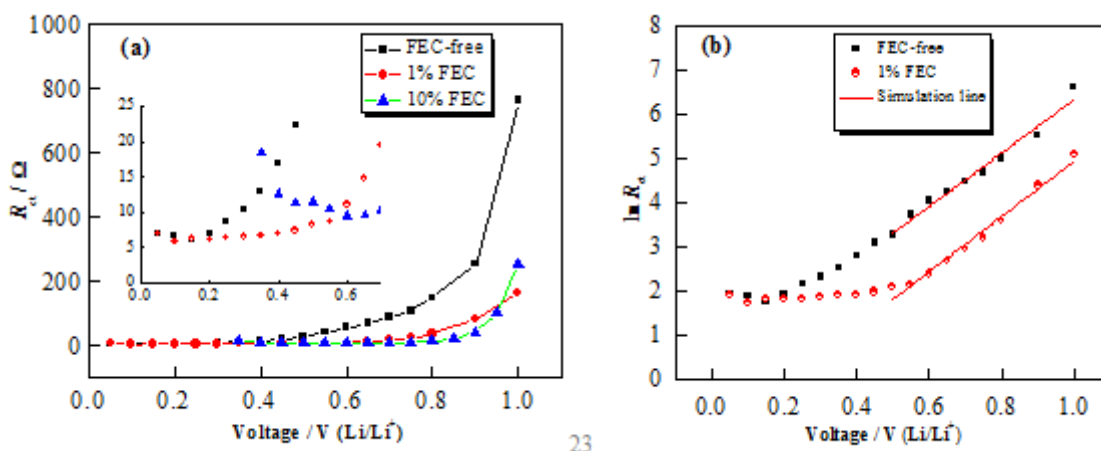


**Figure 12.** Variations of (a)  $R_{ct}$  with the electrode potential in FEC-free, 1% FEC and 10% FEC electrolytes and (b)  $\ln R_{ct}$  in FEC-free and 1% FEC

Fig. 12 reflect the dependence of  $R_{ct}$  on the electrode potential in FEC-free and FEC-containing electrolytes. As can be seen from Fig. 12(a), for the electrolytes without and with 1 % FEC,  $R_{ct}$  decreases with the decrease of electrode polarization potential from 1.0 to 0.5 V during the first lithium ion insertion process and  $R_{ct}$  essentially has a small value below the potential of 0.4 V. However,  $R_{ct}$  is smaller in 1% FEC than that in FEC-free electrolyte electrolyte, indicating that it is easier for lithium ions to insert into and extract from the graphite electrode in FEC-containing electrolyte. In 10 % FEC electrolyte,  $R_{ct}$  decreases in the potential range from 3.0 to 0.6 V, but it increases as the decrease of the potential from 0.6 to 0.35 V, and the semicircle attributed to charge transfer process as shown in Fig. 9 (d) can not be distinguished, which indicates that the charge transfer process has been seriously affected, and it is more difficult for lithium ions to insert into and extract from the graphite electrode, similar to the result of vinylene carbonate (VC) reported by Burns et al. [57].

According to our previous study [58],  $\ln R_{ct}$  can be written as:

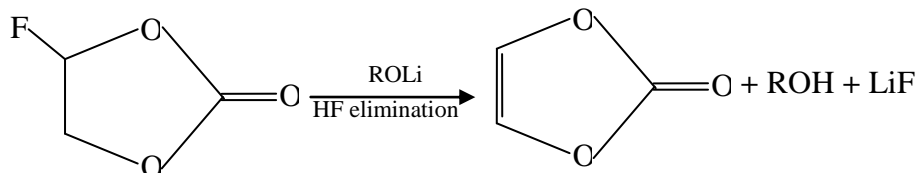
$$\ln R_{ct} = \ln \frac{RT}{n^2 F^2 c_{\max} k_0 (M_{Li^+})^{(1-\alpha)}} - \alpha f(E - E_0)$$

Where  $R$  and  $T$  represent the thermodynamic constant and temperature, respectively,  $n$  is the number of electrons exchanged on the processes of lithium-ion insertion and extraction,  $F$  is the Faraday constant,  $c_{\max}$  (mol/cm<sup>3</sup>) is the maximum concentration of lithium ion in graphite electrode,  $M_{Li}^+$  is the concentration of lithium ion in the electrolyte near the electrode,  $k_0$  represents the standard reaction speed constant,  $E$  and  $E_0$  define the electrode's real and standard potentials, and  $\alpha$  is representing symmetry factor for the electrochemical reaction.

It can be seen that  $R_{ct}$  decreases in an exponential manner with the decreasing of potential when the insertion level  $x \rightarrow 0$ , which coincides with our simulation data, just as shown in Fig. 12(b).  $\ln R_{ct}$  has been linear with the electrode potentials in the potential region from 0.9~0.5 V in the first lithium ion insertion process in both FEC-free and 1% FEC electrolytes. Also, the symmetry factor,  $\alpha$ , can be calculated from the slope of the simulation line. The calculated values of  $\alpha$  in FEC-free and FEC-containing electrolytes are 0.1552 and 0.1603, respectively, implying that the reversibility of charge transfer reaction during the lithium ion insertion and extraction processes has been improved in FEC-containing electrolyte.

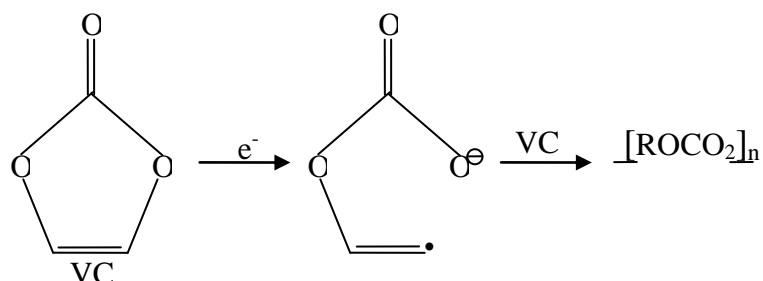
#### 4 DISCUSSION

FEC[33,59] is an interesting compound that itself does not contain vinyl group, however, it can form a VC molecule with losing a HF molecule and provide F<sup>-</sup> to form LiF to as below[28,60]:

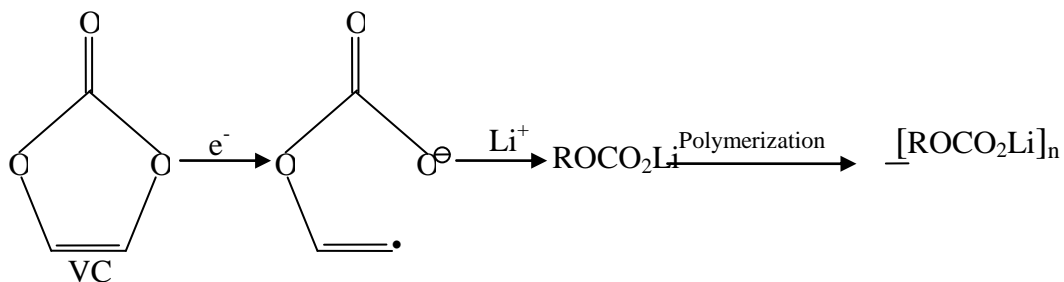


Then VC in turn severs as a polymerizable additive, and there are two reaction pathways of polymerization as below[61,62]:

(1) the first reaction pathway [28]



(2) the second reaction pathway[63]



If the resulting VC polymerize mainly via the first reaction pathway, SEI film composed of purely charge-neutral oligomer products which do not contain  $Li^+$  would be leak of  $Li^+$  conductivity. Moreover,  $Li^+$  diffusion in  $Li_2CO_3$  and  $Li_2O$  was as fast as in graphite, but more difficult in LiF[64,65]. Then, it can be deduced that the SEI film resistance in the FEC-containing electrolyte must be higher than that in the FEC-free electrolyte. On the contrary, as can be seen from EIS results shown in Fig. 11, the SEI film resistance in the FEC-containing electrolyte is lower than that in the FEC-free electrolyte. Thus, it can be concluded that the resulting VC polymerize mainly via the second reaction pathway, and the reaction products is an electrochemically and structurally stable polymers with better  $Li^+$  conductivity, the SEI film containing these polymers is expected to be more cohesive and flexible, and thus provide better passivation than the SEI film comprising only Li salts[66]. Furthermore, concomitant with the formation of VC, LiF is produced from the elimination of HF from FEC and becomes an important component of the SEI film as shown in XPS results. These compounds which do not decompose due to the high bonding energy, are prohibitive to electronic conduction and have a lower solubility in the electrolyte, may be also an important reason for maintaining the stable interface on extending the cycle life [26]. As a result, the performance of graphite electrode in the FEC-containing electrolyte is improved.

In the electrolyte with higher contents of FEC (3 %, 5 % and 10 %), more inorganic components (LiF) appear in the SEI film as shown in SEM and XPS results. In the first Li-ions insertion process, the volume expansion of the graphite particles as Li insertion proceeds, and this expansion is expected to stretch the surface films at the edge planes of the graphite particles through which Li-ions are inserted during the course of Li intercalation and volume expansion[66]. More LiF precipitants that cannot be regarded as being flexible materials in the electrolyte with higher contents of FEC, will result in the decrease of the cohesion and flexibility of the SEI film, and the SEI film can not accommodate the volume expansion. As a result, the initially formed SEI film is cracked because of the expansion of the graphite particles, the electrolyte species permeate and repair the damaged SEI film. The cracking-repairing processes lead to increase in the SEI films' impedance and thickness, in accordance with the EIS results that the resistance of the SEI film increases in the 10% FEC electrolyte more rapidly than that in the FEC-free and 1% FEC electrolyte. More importantly, the volume expansion of the graphite particles upon lithiation-delithiation may be suppressed due to the decrease of the cohesion and flexibility of the SEI film, and then it is more difficult for lithium ions to intercalate into and deintercalate from the graphite electrode in the electrolyte with higher contents of FEC, as evidenced by EIS results. Hence, the major failure mechanism of graphite electrode in the

electrolyte with higher contents of FEC is due to The SEI film comprising more LiF precipitants which result in the decrease of the cohesion and flexibility of the SEI film.

## 5. CONCLUSIONS

This report has discussed the content effect of the electrolyte additive, fluoroethylene carbonate, on cycling performance of mesophase-pitch-based carbon fibers electrode in EC-based electrolyte. Increasing the FEC concentration resulted in improved cycling performance and electrolyte conductivity up to 1 vol%. It was shown that FEC can lose a HF molecule to form a VC molecule and lead to rapid release of F<sup>-</sup> to form LiF, the resulting VC polymerize mainly via the second reaction pathway, and its polymerization products combining with LiF can provide better passivation for graphite electrode, leading to the improved performance of graphite electrode in the FEC-containing electrolyte.

However, as the FEC concentration increased above 3 vol%, the cycling performance and reversible capacity of graphite electrode take a turn for the worse. It was revealed that the SEI film comprising more LiF precipitants which result in the decrease of the cohesion and flexibility of the SEI film can not accommodate the volume expansion of graphite electrode upon lithiation-delithiation, leading to larger charge transfer instance and SEI film resistance, and then the deterioration of electrochemical performance of graphite electrode.

It is clear that FEC is a beneficial additive for the improvement of electrochemical performance of graphite electrode, however, when choosing FEC as a film-forming additives, we must control the amount of FEC in the electrolyte to achieve the best effect of improvement, and 1.0 vol % FEC may be the appropriate content.

## ACKNOWLEDGEMENTS

This work was partly supported by the Fundamental Research Funds for the Central Universities (2013XK07) and Jiangsu province ordinary university graduate student research innovation project (CXZZ13\_0952)

## References

1. J. A. Carpenter, J. Gibbs, A. A. Pesaran, L. D. Marlino, K. Kelly, *MRS Bull.* 33 (2008) 439.
2. J. M. Tarascon, M. Armand, *Nature* 414 (2001) 359.
3. M. Armand, J.-M. Tarascon, *Nature* 451 (2008) 652.
4. H. H. Zheng, K. Jiang, T. Abe, Z. Ogumi, *Carbon* 44 (2006) 203.
5. S. S. Zhang, *J. Power Sources* 162 (2006) 1379.
6. P. Verma, P. Maire, P. Novák, *Electrochim. Acta* 55 (2010) 6332.
7. K. Xu, *Chem. Rev.* 104 (2004) 4303.
8. D. Aurbach, Y. Ein-Eli, O. Cifusid, *J. Electrochem. Soc.* 141 (1994) 603.
9. H. Buqa, A. Würsig, J. Vetter, M. E. Spahr, F. Krumeich, P. Novák, *J. Power Sources* 153 (2006) 385.

10. D.Aurbach, K. Gamolsky, B. Markovsky, Y. Gofer, M. Schmidt, U. Heider, *Electrochim. Acta* 47 (2002)1423.
11. L. Chen, K. Wang, X. Xie, J. Xie, *J. Power Sources* 174 (2007) 538.
12. Y. Ein-Eli, S. R. Thomas, V. R. Koch, *J. Electrochem. Soc.* 144 (1997) 1159.
13. J. S. Shina, C. H. Hana, U. H. Jung, *J. Power Sources* 109 (2002) 47.
14. Y. K. Choi, K. Chung, W. S. Kim, *J. Power Sources* 104 (2002) 132.
15. K. Chung, J. D. Lee, E. J. Kim, WS Kim, J. H. Cho,Y. K. Choi, *Microchem. J.* 75 (2003) 71.
16. H. Zheng, Y. Fu, H. Zhang, *Electrochim. Solid -State Lett.* 9 (2006) A115.
17. Q. C. Zhuang, J. Li, L. L. Tian, *J. Power Sources* 222 (2013) 177.
18. G. H. Wrodnigg, J. O. Besenhard, M. Winter, *J. Electrochem. Soc.* 146 (1999) 470.
19. G. H. Wrodnigg, T. M. Wrodnigg, J. O. Besenhard, M. Winter, *Electrochim. Commun.* 1 (1999) 148.
20. W. Yao, Z. Zhang, J. Gao, *Energy Environ. Sci.* 2 (2009) 1102.
21. Y.S. Hu, W. Kong, H. Li, *Electrochim. Commun.* 6 (2004) 126.
22. Y.S. Hu, W. Kong, Z. Wang, *Electrochim. Solid-State Lett.* 7 (2004) A442.
23. T.H. Nam, E.G. Shim, J.G. Kim, H. S.Kim, S. I. Moon, *J. Electrochem. Soc.* 154 (2007) A957.
24. Y. Fu, C. Chen, C. Qiu, et al., *J. Appl. Electrochem.* 39 (2009) 2597.
25. S. D. Xu, Q. C. Zhuang, J. Wang, Y. Q. Xu, Y. B. Zhu, *Int. J. Electrochem. Sci.* 8 (2013) 8058
26. M. H. Ryou, G. B. Han, Y. M. Lee, *Electrochim. Acta*, 55 (2010) 2073.
27. N. S. Choi, Y. Lee, S.S. Kim, *J. Power Sources* 195 (2010) 2368.
28. V. Etacheri, O. Haik, Y. Gofer, G. A. Roberts, I. C. Stefan, R. Fasching, D. Aurbach, *Langmuir* 28 (2012) 965.
29. N. S. Choi, K. H. Yew, K. Y. Lee, M. Sung, H. Kim, S.-S. Kim, *J. Power Sources* 161 (2006) 1254.
30. J. Xu, W.-H. Yao, Y.-W. Yao, *Acta Phys.-Chim. Sin.* 25 (2009) 201.
31. I. Profatilova, S. S. Kim, N. S. Choi, *Electrochimica Acta* 54 (2009) 4445.
32. J. H. Song, J. T. Yeon, J. Y. Jang, *J. Electrochem. Soc.* 160 (2013) A873.
33. R. McMillan, H. Slegr, Z. X. Shu, W.Wang, *J. Power sources* 81-82 (1999) 20.
34. C. Jung, *Solid State Ionics* 179 (2008) 1717.
35. S. A. Webb, L. Baggetto, C. A. Bridges, *J. Power Sources* 248 (2014) 1105.
36. E. Barsoukov , J. H. Kim, C. O. Yoon, *Solid State Ionics* 116 (1999) 249.
37. E. Barsoukov, J.H. Kim, C. O. Yoon, *J. Electrochem. Soc.* 145 (1999) 2711.
38. D. Aurbach, M.D. Levi, E. Levi, *J. Phys. Chem. B* 101 (1997) 2195.
39. T. Piao, S. M. Park, C. H. Doh, S. I. Moon, *J. Electrochem. Soc.* 146 (1999) 2794.
40. A. Funabiki, M. Inaba, Z. Ogumi, *J. Power Sources* 68 (1997) 227.
41. S. Zhang, P. Shi, *Electrochim. Acta* 49 (2004) 1475.
42. J. S. Kim, Y. T. Parkr. *J. Power Sources* 91(2000)172.
43. S. S. Zhang, K. Xu, T. R. Jow. *J. Power Sources* 130 (2004) 281.
44. A. Naji, J. Ghanbaja, P. Willmann, B. Humbert, D. Billaud, *J. Power Sources* 62 (1996) 141.
45. A. Naji, J. Ghanbaja, B. Humbert, P. Willmann, D. Billaud, *J. Power Sources* 63 (1996) 33.
46. Y. B. Liu, L. Tan, L. Li, *J. Power Sources* 211 (2013) 90.
47. I. A. Profatilova, S. S. Kim, N. S. Choi, *Electrochim. Acta*, 54(2009) 4445.
48. X. Y. Qiu, Q. C. Zhuang, Q. Q. Zhang, R. Cao, P. Z. Ying, Y. H. Qiang, S. G. Sun, *Phys. Chem. Chem. Phys.* 14 (2012) 2617.
49. Q. C. Zhuang, T. Wei, L. L. Du, Y. L. Cui, L. Fang, S. G. Sun, *J. Phys. Chem. C* 114 (2010) 8614.
50. M. Holzapfel, A. Martinent, F. Alloin, B. L. Gorrec, R. Yazami, C. Montella, *J. Electroanal. Chem.* 546 (2003) 41.
51. Y. C. Chang, H. J. Sohn, *J. Electrochem. Soc.* 147 (2000) 50.
52. D. Aurbach, *J. Power Sources* 89 (2000) 206.

53. D. Aurbach, M. D. Levi, E. Levi, H. Teller, B. Markovsky, G. Salitra, U. Heider, L. Heider, *J. Electrochem. Soc.* 145 (1998) 3024.
54. M. D. Levi, D. Aurbach, *J. Phys. Chem. B* 101 (1997) 4630.
55. S. D. Xu, Q. C. Zhuang, L. L. Tian, Y. P. Qin, L. Fang, S. G. Sun, *J. Phys. Chem. C* 115 (2011) 9210.
56. L. L. Tian, Q. C. Zhuang, J. Li, Y. L. Yue, J. P. Chen, F. Lu, S. G. Sun, *Chinese Science Bulletin* 56 (2011) 3204.
57. J. C. Burns, R. Petibon, K. J. Nelson, *J. Electrochem. Soc.* 160 (2013) A1668.
58. C. Wang, I. Kakwan, A. J. Appleby, *J. Electroanal. Chem.* 489 (2000) 55.
59. R. Mogi, M. Inaba, S. K. Jeong, Y. Iriyama, T. Abe, Z. Ogumi, *J. Electrochem. Soc.* 149 (2002) A1578.
60. K. Leung, S. B. Rempe, M. E. Foster, *J. Electrochem. Soc.*, 161 (2014) A213.
61. B. M. Trost, Z. T. Ball, T. Joge, *J. AM. CHEM. Soc.* 124 (2002) 4408.
62. X. L. Chen, X. L. Li, D. H. Mei, *Chem Sus Chem* 7 (2014) 549.
63. H. H. Lee, Y. Y. Wang, C. C. Wan, *J. Appl. Electrochem* 35 (2005) 615.
64. H. Iddir, L. A. Curtiss, *J. Phys. Chem. C* 114 (2010) 20903.
65. K. Tasaki, S. J. Harris, *J. Phys. Chem. C* 114 (2010) 8076.
66. M. Koltypin. *Electrochem. Commun.* 4 (2002) 17.

© 2015 The Authors. Published by ESG ([www.electrochemsci.org](http://www.electrochemsci.org)). This article is an open access article distributed under the terms and conditions of the Creative Commons Attribution license (<http://creativecommons.org/licenses/by/4.0/>).